6268 *J. Am. Chem. Soc.* **1993,** *115,* 6268–6276

Reactions of Transition-Metal Ions with Sulfur Hexafluoride in the Gas Phase

Charles Q. Jiao and Ben S. Freiser*

Contribution from the Department of Chemistry, Purdue University, West Lafayette, Indiana 47907

Received July 27, 1992. Revised Manuscript Received January 6, 1993

Abstract: The inertness of SF_6 is well-known to be associated with the protective layer of F atoms which obstructs the access to the reactive S center by an attacking species. Previous gas-phase studies of SF_6 involved reactants having high ionization energies, such as He^+, Ar^+, and N_2^+, which are observed to yield predominantly SF_5^+ either via F^- abstraction or dissociative charge transfer. This study shows that early transition metal ions, despite their low ionization potentials, can react with SF_6 yielding product distributions much different from those of the reactions studied previously. In contrast, the reduced reactivity and mainly absence of reactivity observed for the late transition metal ions indicates that an empty d orbital is required for reaction. Rate constants for some selected early transition metal ion reactions are determined. Sc^+ was chosen to be studied in detail because a complete set of thermodynamic data on $ScF_n^{+/0}$ were available in the literature. The reaction pathways are derived and a reaction mechanism involving oxidative addition is proposed.

I. Introduction

The study of sulfur hexafluoride has been of great interest for several decades. Many of its properties have been investigated with practical applications in mind. Among the most important examples are its applicability for isotope separation by laser irradiation[1,2] and its use as a source of F atoms in lasers, as well as in plasma etching processes.[3,4] For its high chemical stability and excellent insulating properties, it has been widely used in the electrical transmission industry as a highly efficient insulator of high-voltage equipment.[5] In addition, it has also attracted much attention from chemists interested in fundamental questions. For example, SF_6 has been considered as a model[6] representing in many respects the kind of bonding in hypervalent compounds which exceeds the number of valences permitted on the basis of the Langmuir–Lewis theory of bonding.[7] Extensive theoretical calculations[8] and experimental research[9] on various aspects of SF_6, including ionization energies and electronic structure, have been carried out over the past 20 years. Whether the 3d orbitals in the S atom participate in the bonding orbitals or not is in question, since they are so diffuse that their overlap with the bond orbitals of the fluorides is too small to make a significant contribution to molecular binding. Furthermore, the promotion energy for transferring one s- and one p-electron in the S atom into an empty d orbital is rather high.[7,10] A number of explanations, based on either valence bond[6,7,11] or molecular orbital theory,[6,7,11,12] have been proposed to elucidate the bonding nature of this kind of molecule.

Experimental studies on the reactivity of SF_6 with various chemical species should lead to a better understanding of the bonding nature of this molecule. Sulfur hexafluoride, however, is almost inert to both nucleophilic and electrophilic reagents.[13] It is unaffected by aqueous solutions of fused alkali, ammonia, or oxygen.[14] It is attacked readily only by powerful reagents, such as sodium in liquid NH_3,[13] and strong Lewis acids.[15] It is not surprising, therefore, that most of its reactions which have been well-studied occur in the area of gas-phase ion–molecule reactions, where the reactant cations act as the Lewis acids. Table I summarizes the previously studied reactions of SF_6 with various ionic species. The product ion is exclusively SF_5^+ in all cases except He^+ and Xe^+. The SF_6^+ ion is not found in the products because it is unusually unstable and fragments to SF_5^+.

The behavior of SF_6 in these reactions can be understood in terms of its structure. The S–F bond energy in SF_6 differs little from that in SF_4, but the latter is rather reactive while the former is not. Thus, it has been suggested that the inertness of SF_6 must be kinetic rather than thermodynamic.[14] The stability has been considered to be associated with the protective layer of fluorine atoms surrounding the central sulfur atom.[8] In this fully space-filled molecule, access to the reactive center by an attacking species is obstructed, in contrast to SF_4 (incomplete trigonal-bipyramidal structure) where the sulfur is accessible. Thus, it can be expected that SF_6 will undergo reactions in which the S atom is not attacked directly. In the ion–molecule reactions given in Table I, the reaction mechanisms involve either charge transfer to form an unstable $[SF_6^+]^*$, followed by fragmentation to SF_5^+ (eq 1),[16] or F^- abstraction (eq 2).[17]

dissociative charge-transfer:

$$\begin{aligned} &X^+ + SF_6 \longrightarrow \\ &\qquad X + [SF_6^+]^* \\ &\qquad\quad \hookrightarrow F + SF_5^+ \qquad (1) \end{aligned}$$

F^- abstraction:

$$X^+ + SF_6 \longrightarrow XF + SF_5^+ \qquad (2)$$

When X has a sufficiently high ionization potential (IP), SF_5^+

---

(1) Lyman, J. L.; Jensen, R. J. *J. Phys. Chem.* **1973,** *77,* 883.

(2) Chen, C. L.; Chantry, P. J. *J. Chem. Phys.* **1979,** *71,* 2897.

(3) Flamm, D. L.; Donelly, V. M. *Plasma Chem. Plasma Process* **1981,** *1,* 317.

(4) Cob, J. W. *Plasma Chem. Plasma Process* **1982,** *2,* 1.

(5) Griffiths, W. J.; Harris, F. M. *Int. J. Mass Spectrom. Ion Processes* **1988,** *85,* 259.

(6) Mitchell, K. A. *Chem. Rev.* **1969,** *69,* 157.

(7) Pauling, L. *The Nature of The Chemical Bond,* 3rd ed.; Cornell University Press: Ithaca, NY, 1960.

(8) (a) Tand, R.; Callaway, J. *J. Chem. Phys.* **1986,** *84,* 6854. (b) Gutsev, G. L.; Klyagina, A. P. *Chem. Phys.* **1983,** *75,* 243. (c) Lazzeretti, P.; Pincelli, U.; Rossi, E.; Zanasi, R. *J. Chem. Phys.* **1983,** *79,* 4085.

(9) (a) Potts, A. W.; Lempka, H. J.; Streets, D. G.; Price, W. C. *Philos. Trans. R. Soc. London, A* **1970,** *268,* 59. (b) Dehmer, J. L. *J. Chem. Phys.* **1972,** *56,* 4496. (c) Lavilla, R. E. *J. Chem. Phys.* **1972,** *57,* 899. (d) Gelius, U. *J. Electron Spectrosc.* **1974,** *5,* 985. (e) Sell, J. A.; Kuppermann, A. *Chem. Phys.* **1978,** *33,* 379. (f) Stone, J. A.; Wytenberg, W. J. *Int. J. Mass Spectrom. Ion Processes* **1989,** *94,* 269. (g) Sieck, L. W.; Ausloos, P. J. *J. Chem. Phys.* **1990,** *93,* 8374. (h) Fisher, E. R.; Kickel, B. L.; Armentrout, P. B. *J. Chem. Phys.* Submitted for publication.

(10) Coulson, C. A. *Valence*; Oxford University Press: London, 1961.

(11) Coulson, C. A. *J. Chem. Soc., London* **1964,** 1442.

(12) (a) Rundle, R. E. *Surv. Prog. Chem.* **1963,** *1,* 81. (b) Musher, J. I. *Angew. Chem.* **1969,** *81,* 68. (c) Jorgensen, C. K. *Struct. Bonding (Berlin)* **1969,** *6,* 94.

(13) Demitras, G. C.; MacDiarmid A. G. *Inorg. Chem.* **1964,** *3,* 1198.

(14) Roberts, H. L. *Q. Rev. (London)* **1961,** *15,* 30.

(15) Case, J. R.; Nyman, F. *Nature* **1962,** *193,* 473.

(16) Babcock, L. M.; Streit, G. E. *J. Chem. Phys.* **1981,** *74,* 5700.

(17) Tichy, M.; Javahery, G.; Twiddy, N. D. *Int. J. Mass-Spectrom. Ion Processes* **1987,** *79,* 231.

0002-7863/93/1515-6268$04.00/0

Table I. Previously Studied Reactions of SF_6 with Some Ionic Species

reactions[a]	$AP(SF_5^+/SF_6) - IP(M)$[b] (eV)	$10^{10}k$ (cm^3 $molecule^{-1}$ s^{-1})	ref
$SF_5^+ + F + He$		20	16, 38
$SF_6 + He^+ \rightarrow$ $SF_4^+ + 2F + He$	−10.18	20	16, 38
$SF_3^+ + 3F + He$			
$SF_6 + Ar^+ \rightarrow SF_5^+ + F + Ar$	−1.78	9.3	22
		9	39
		12	38
$SF_6 + HCl^+ \rightarrow SF_5^+ + HF + Cl$	−1.23	12.5	17
$SF_6 + N_2^+ \rightarrow SF_5^+ + F + N_2$	−1.16	13	16, 38
$SF_6 + Kr^+ (P_{1/2}) \rightarrow SF_5^+ + F + Kr$	−0.70		16
		0.3	39
$SF_6 + Ar_2^+ \rightarrow SF_5^+ + F + 2Ar$	−0.52	4.2	38
$SF_6 + CF_3^+ \rightarrow SF_5^+ + CF_4$	−0.17		16
$SF_6 + N^+ \rightarrow SF_5^+ + FN$	−0.11	14	16, 38
$SF_6 + Kr^+ (P_{3/2}) \rightarrow SF_5^+ + F + Kr$	−0.02	6	39
$SF_6 + CO^+ \rightarrow SF_5^+ + COF$	+0.03	13	38
$SF_6 + O^+ \rightarrow SF_5^+ + OF$	+0.36	15	38
$SF_6 + CO_2^+ \rightarrow SF_5^+ + CO_2F$	+0.65	0.14	16
$SF_6 + Xe^+_{3/2} \rightarrow SF_3^+ + XeF_2 + F$	+1.20	<0.05	39
$SF_6 + O_2^+ \rightarrow SF_5^+ + FO_2$	+1.91	<0.1	38
$SF_6 + SO_2^+ \rightarrow SF_5^+ + SO_2F$	+2.08	2.8	16
$SF_6 + C^+ \rightarrow SF_5^+ + CF$	+2.27	13	38
$SF_6 + H_3O^+ \rightarrow$ no reaction		<0.05	16
$SF_6 + NO_2^+ \rightarrow$ no reaction	+4.67	<0.05	16
$SF_6 + NO^+ \rightarrow SF_5^+ + NOF$	+4.72[c]	<0.1	38
$SF_6 + NO^+ \rightarrow$ no reaction	+5.16[c]	<0.05	16

[a] Most likely neutral products are shown. [b] For the reactions of SF_6 with CO^+, O^+, CO_2^+, and SO_2^+ etc., the energetics require that there be some bond formation in the products since $AP(SF_5^+/SF_6) - IP(M)$ is positive and since the product ion observed is SF_5^+. [c] These two different values are cited from each reference given.

can fragment further to SF_4^+ and SF_3^+, as in the case of the He^+ reaction shown in Table I. Furthermore, when the energy of the impacting electrons used to generate He^+ is increased, more SF_3^+ is produced, arising from an increased population of electronically excited He^+.[16]

The reaction enthalpies for the charge-transfer reaction (ΔH_1) and the F^- abstraction (ΔH_2) are respectively

$$\Delta H_1 = AP(SF_5^+/SF_6) - IP(X)$$

$$\Delta H_2 = [AP(SF_5^+/SF_6) - D(XF)] - IP(X)$$

For these reactions to take place with observable reaction rates, the ionization potential (IP) of X must be greater than the appearance potential of SF_5^+ from SF_6, $AP(SF_5^+/SF_6)$, for reaction 1 or greater than $[AP(SF_5^+/SF_6) - D(XF)]$ for reaction 2, where $D(XF)$ is the X–F bond energy. Table I also lists the values of $AP(SF_5^+/SF_6) - IP(X)$ for each reaction along with the reaction rate constants. For reactions which would be endothermic in the absence of bond formation between X and F, the neutral XF products are shown and the X–F bond energies are sufficient to make the reactions exothermic.[16]

Despite the extensive literature on the gas-phase chemistry of metal ions,[18] few studies have involved SF_6. Metal species generally have low ionization potentials and, thus, cannot react with SF_6 by reaction 1 or 2 exothermically (as listed in Table II for some selected transition metal ions, the reaction enthalpies for eqs 1 and 2 are all positive). In an earlier study, however, we reported that Ti^+, despite its IP (6.82 eV) being far below the value of $AP(SF_5^+/SF_6)$ (14.62 eV),[16] reacts readily with SF_6 to give a striking product pattern, with SF_3^+ being the predominant ion, and SF_2^+ and SF_4^+ each having significant intensities.[19] In addition, TiF_n^+ (n = 1–3) products are also generated.

Here we describe an extension to this earlier work with an investigation of the reactions of SF_6 with a variety of transition metal ions, focussing on the reactions of SF_6 with Sc^+. This system was chosen first, since complete thermodynamic data were available in the literature on ScF_n (n = 1–3) and ScF_n^+ (n = 1, 2), permitting reaction pathways to be derived from the results of both experiments and thermodynamic calculations. In addition Sc^+ has been studied with a variety of reagent gases.[20] The relationship between reaction branching ratios and reaction enthalpies is discussed, and a reaction mechanism involving oxidative addition is proposed.

II. Experimental Section

All experiments were performed on a Nicolet FTMS-2000 dual cell Fourier transform ion cyclotron resonance mass spectrometer.[21] Metal ions were trapped and reacted with SF_6 in a 4.9 cm^3 cell located in the analyzer region of the FTMS-2000. This cell was immersed in a 3 T magnetic field, and trapping potentials were maintained at 2 V. The sulfur hexafluoride was introduced via a leak valve, and the pressure used ranged from 1.5×10^{-7} to 2.5×10^{-7} Torr for the early transition metal ions and from 2.5×10^{-7} to 9.1×10^{-6} Torr for the late transition metal ions.

Chemicals were obtained commercially in high purity and used as supplied except for multiple freeze–pump–thaw cycles to remove noncondensable gases. A Bayard-Alpert ionization gauge was used to monitor pressure. The number density (pressure) of SF_6 was calibrated by measuring the reaction rate (s^{-1}) of Ar^+ with SF_6 and dividing by a literature value for the rate constant of 9.3×10^{-10} cm^3 $molecules^{-1}$ s^{-1}.[22] A static background pressure of argon at 2×10^{-6} Torr served as the collision gas for collision-induced dissociation (CID) experiments.[21c]

To determine parent–product ion relationships, the techniques of ion isolation and continuous ejection were used.[21c,23a] One possible complication which may arise when performing continuous ejection of an unwanted ion is off-resonance excitation of the ion of interest. This would result in a change in its kinetic energy, thus affecting its reactivity. The

---

(18) Eller, K.; Schwarz, H. *Chem. Rev.* **1991**, *91*, 1121.

(19) Burnier, R. C.; Bird, G. D.; Carlin, T. J.; Wise, M. B.; Cody, R. B.; Freiser, B. S. *Lecture Notes in Chemistry*; Hartmann, H., Wanczek, K.-P., Eds.; Springer-Verlag: New York, 1982.

(20) (a) Tolbert, M. A.; Beauchamp, J. L. *J. Am. Chem. Soc.* **1984**, *106*, 8117. (b) Lech, L. M.; Freiser, B. S. *Organometalics* **1988**, *7*, 1948. (c) Sunderlin, L.; Aristov, N.; Armentrout, P. V. *J. Am. Chem. Soc.* **1987**, *109*, 78.

(21) For a review of Fourier transform mass spectrometry, see: (a) Wanczek, K. P. *Int. J. Mass Spectrom. Ion Processes* **1989**, *95*, 1. (b) Marshall, A. G.; Verdun, F. R. *Fourier Transform in NMR Optical and Mass Spectrometry*; Elsevier: Amsterdam, 1990; Chapter 7. (c) Freiser, B. S. In *Techniques for the study of Ion Molecule Reactions*; Farrar, J. M., Saunder, W. H., Jr., Eds.; Wiley: New York, 1988; Vol. 20, Chapter 2.

(22) Shul, R. J.; Upschulte, B. L.; Passarella, R.; Keesee, R. G.; Castleman, A. W., Jr. *J. Phys. Chem.* **1987**, *91*, 2556.

phenomenon of off-resonance excitation has been discussed in depth by Jacobson and co-workers in its application to perform very low energy (<5 eV) collision-induced dissociation.[23b] The maximum kinetic energy ($E_{\mathrm{tr(max)}}$) of an ion induced by off-resonance excitation is readily calculated from

$$E_{\mathrm{tr(max)}} = \frac{E^2e^2}{16m\pi^2}\frac{1}{\Delta f^2}$$

where E is the radio-frequency electric field strength and Δf is the difference between the natural cyclotron frequency of the ion and the applied radio frequency. The inverse squared relationship of Δf means that $E_{\mathrm{tr(max)}}$ drops off rapidly as the radio frequency is applied further from the cyclotron frequency. In this study, the most extreme case, i.e., the smallest Δf used, involved monitoring ScF_2^+ while continuously ejecting SF_3^+ in which Δf = 38.4 kHz. With the radio-frequency amplitude of 3.64 V used in these experiments, the maximum translational energy of ScF_2^+ is calculated to be only 0.028 eV or very nearly room temperature. Therefore, we believe that off-resonance excitation has had no significant effect on the determinations of product ratios and rate constants.

For most of the reactions, the number of data points used for sampling the profile of the image current was 16K. For the reactions of Y^+ and V^+, however, higher resolution was required to distinguish isobaric ions, such as Y^+ (88.9059 amu) vs SF_3^+ (88.9673 amu), YF_2^+ (126.9027 amu) vs SF_5^+ (126.9641 amu), VF_4^+ (126.9373 amu) vs SF_5^+ (126.9641 amu), and so on. The highest resolution required was $M/\Delta M$ = 4740 to distinguish VF_4^+ from SF_5^+, which is readily achieved using FTMS.[21b] In these cases, the number of sampling data points used was 256K, yielding a resolution of about 8000 at m/z 127.

The metal ions were generated by focusing the fundamental output (1064 nm) of a Q-switched Nd:YAG laser onto a selected pure metal target.[24a] The metal targets are supported on a flange of a four-way cross which extends from the analyzer region and is external to the solenoid magnet.[24b] The magnetic field focusses a portion of the ions down the center of the chamber, and no additional extraction or focussing optics are required to achieve intense metal ion signals in the analyzer cell.

Metal ions generated by laser desorption have a broad distribution of kinetic energies.[25] Although ions having axial kinetic energies much greater than 2 eV will not be trapped efficiently using 2 V trapping potentials, ions having relatively low axial kinetic energy but entering off-axis may be excited substantially in their cyclotron motion. It has been our experience, and additional evidence is presented in this work, that the ions become kinetically thermalized when they are trapped for 1 s in the presence of 2 × 10^{-6} Torr of Ar introduced via a leak valve.

While the kinetic energy distributions for laser desorbed metal ions have been well-characterized,[25] the electronic state distributions have not. This is due in part to the fact that most reports of excited ion chemistry cannot readily distinguish between electronically and translationally excited species.[26] In contrast, for electron impact ionization (EI), the electronic state distributions for some metal ions have been well-characterized[27] and it is now known that a significant fraction of most metal ions produced by EI of transition-metal compounds are formed in long-lived (seconds) metastable states.[27h,i] By using EI to generate the metal ions, Armentrout studied the state-specific gas-phase ion–molecule reactions of the first-row transition-metal ions.[26] Bowers has developed an elegant gas-phase chromatographic method to quantitate the electronic configuration of the first-row transition-metal ions, the deactivation of electronically excited states by collision with helium, and the state-specific clustering equilibrium with helium.[28] Other methods for producing a well-defined population of electronic states include surface ionization whereby the electronic state populations can be controlled by changing the filament temperature[29] and multiphoton ionization which was developed by Weisshaar for the study of transition metal ion chemistry.[30]

In our study, although no doubly charged metal ions were generated under the laser desorption conditions used (with a laser power density of about 2 × 10^8 W cm^{-2}), some of the singly-charged metal ions were almost certainly born in electronically excited states during the 10-ns laser pulse. However, no evidence was found in this study to suggest that they were in sufficient concentration or sufficiently long-lived to play a dominant role in the reactivity observed.[31] In particular following the 1 s thermalization period, either the entire metal ion population was unreactive or, if they did react, they exhibited single exponential behavior to over 3 half-lives. It is highly unlikely that in each case the excited metal ions decay at the same rate as the ground state ion or, conversely, that no ground state was present. Furthermore, the reactivity of Sc^+ was not observed to change following a 30 s trapping period (in the presence of Ar at 6.2 × 10^{-7} Torr) to permit additional collisional and radiative decay. Thus, we believe that electronically excited states play little, if any, role in the observed chemistry.

III. Results and Discussion

SF_6 was reacted with some selected transition-metal ions as listed in Table II. In each case, reactions were studied with both "hot" metal ions (i.e., the metal ions were reacted with SF_6 directly after being generated without being collisionally cooled) and "cooled" metal ions (the metal ions were permitted to undergo thermalizing collisions with Ar gas for 1 s prior to reaction with SF_6). When the metal ions were hot, all of them were observed to react with SF_6, with the early transition metal ions producing SF_n^+ (n = 2–5) and MF_m^+ (m = 1–4) and the late transition metal ions producing only SF_5^+ and SF_3^+, with SF_5^+ usually predominating. When the metal ions were cooled, however, only the early transition metal ions were observed to react, while the late transition metal ions were either unreactive or much less reactive (for example, for the reaction of Fe^+, SF_3^+ and SF_5^+ were still observed, but the reaction rate constant is rather low, <1 × 10^{-11} cm^3 $molecules^{-1}$ s^{-1}, suggesting that either this reaction is slightly endothermic or there is a slight kinetic barrier). Table II lists a survey of the reactivites of the selected transition-metal ions (cooled) with SF_6, along with the ground state electronic configurations. It is evident from Table II that a clear turnover point occurs between group 5 and group 6, indicating that having an empty d orbital facilitates the reaction with SF_6.

The product distributions for the early transition metal ion reactions are shown in Table III. The data were obtained with a reaction time of 1 s and at the pressure of SF_6 indicated in the table. Results from both "hot" ion and "cooled" ion reactions are presented. It can be seen that the percentage of SF_5^+ increases significantly when the metal ions are hot. This is in contrast to the reaction of He^+ mentioned above where, when He^+ is electronically excited, the SF_5^+ intensity decreases and the SF_3^+

---

(23) (a) Comisarow, M. B.; Parisod, G.; Grassi, V. *Chem. Phys. Lett.* **1978**, *57*, 413. (b) Gauthier, J. W.; Trautman, T. R.; Jacobson, D. B. *Anal. Chim. Acta* **1991**, *246*, 211.

(24) (a) Cody, R. B.; Burnier, R. C.; Reents, W. D.; Carlin, T. J.; McCrery, D. A.; Lengel, R. K.; Freiser, B. S. *Int. J. Mass Spectrom. Ion Phys.* **1980**, *33*, 37. (b) Weller, R. R.; MacMahon, T. J.; Freiser, B. S. In *Lasers in Mass Spectrometry*; Lubman, D. M., Ed.; Oxford University Press: New York, 1990; Vol. 1, p 249.

(25) Kang, H.; Beauchamp, J. L. *J. Phys. Chem.* **1985**, *89*, 3364.

(26) Armentrout, P. B. *Annu. Rev. Phys. Chem.* **1990**, *41*, 313.

(27) (a) Elkind, J. L.; Armentrout, P. B. *J. Phys. Chem.* **1985**, *89*, 5626. (b) Elkind, J. L.; Armentrout, P. B. *J. Chem. Phys.* **1986**, *84*, 4862. (c) Elkind, J. L.; Armentrout, P. B. *J. Am. Chem. Soc.* **1986**, *108*, 2765. (d) Elkind, J. L.; Armentrout, P. B. *J. Phys. Chem.* **1986**, *90*, 5736. (e) Elkind, J. L.; Armentrout, P. B. *J. Phys. Chem.* **1986**, *90*, 6576. (f) Elkind, J. L.; Armentrout, P. B. *J. Chem. Phys.* **1987**, *86*, 1868. (g) Elkind, J. L.; Armentrout, P. B. *Int. J. Mass Spectrom. Ion Processes* **1988**, *83*, 259. (h) Reents, W. D., Jr.; Strobel, F.; Freas, R. B., III; Wronka, J.; Ridge, D. P. *J. Phys. Chem.* **1985**, *89*, 5666. (i) Strobel, F.; Ridge, D. P. *J. Phys. Chem.* **1989**, *93*, 3635.

(28) Kemper, P. R.; Bowers, M. T. *J. Phys. Chem.* **1991**, *95*, 5134.

(29) Sunderlin, L. S.; Armentrout, P. B. *J. Phys. Chem.* **1988**, *92*, 1209.

(30) Weisshaar, J. C. In *State-Selected and State-to-State Ion-Molecule Reaction Dynamics, Part 1: Experiment*; Ng, C. Y., Baer, M., Eds.; John Wiley & Sons, Inc.: New York, 1992.

(31) (a) A particular case in point is Cr^+, which is known to contain about 74% excited state when generated by electron impact.[27h] When Cr^+, generated by electron impact, is allowed to react with SF_6, a small amount of CrF^+ and CrF_2^+, as well as SF_n^+ (n = 3–5), is observed. We assign the reactions which form CrF^+ and CrF_2^+ as arising from the excited states of Cr^+ with an empty d orbital (for example, a ^6D, $3d^44s$). In contrast, kinetically hot Cr^+, generated by laser desorption, yields only SF_n^+ (n = 3 and 5) and when thermalized is totally unreactive with SF_6. (b) In the case of Fe^+, Russell and Oriedo have reported that 65% of its population are in the excited states with the energies up to about 4.0 eV when Fe^+ is generated by 50–70 eV electron impact on $Fe(CO)_5$.[44] Using the same methodology, we observed that when Fe^+ is generated by laser desorption followed by a 1 s collisional cooling period at 2 × 10^{-6} Torr of Ar, about 8% are generated in the first excited state and about 3% are in the second to fourth excited states. Under similar conditions the entire population of Fe^+ is observed to react with SF_6, indicating that the ground state of Fe^+ is also reactive forming predominantly SF_3^+.

Table II. Survey of Reactivities of Transition-Metal Ions with Sulfur Hexafluoride Along with the List of the Ground State Electron Configurations[a]

group	M^+	reaction obsd	electron configuration		ΔH_1 (eV)[b]	ΔH_2 (eV)[c]
3	Sc^+	yes	[Ar]4s3d	$^3D_1$	8.08	1.90
3	Y^+	yes	[Kr]5s^2	$^1S_0$	8.28	1.66
3	La^+	yes	[Xe]5d^2	$^3F_2$	9.04	
4	Ti^+	yes	[Ar]4s3d^2	$^4F_{3/2}$	7.80	1.37
4	Zr^+	yes	[Kr]5s4d^2	$^4F_{3/2}$	7.78	1.49
5	V^+	yes	[Ar]3d^4	$^5D_0$	7.88	
5	Nb^+	yes	[Kr]4d^4	$^5D_0$	7.74	
5	Ta^+	yes	[Xe]4f^{14}6s5d^3	$^5F_1$	6.73	
6	Cr^+	no	[Ar]3d^5	$^6S_{5/2}$	7.85	
6	Mo^+	no	[Kr]5d^5	$^6S_{5/2}$	7.52	
7	Mn^+	no	[Ar]4s3d^5	$^7S_3$	7.19	
8	Fe^+	yes[d]	[Ar]5s3d^6	$^6D_{9/2}$	6.75	2.12
9	Co^+	no	[Ar]3d^8	$^3F_4$	6.76	
9	Rh^+	no	[Kr]4d^8	$^3F_4$	7.16	
10	Ni^+	no	[Ar]3d^9	$^2D_{5/2}$	6.99	
10	Pd^+	no	[Kr]4d^9	$^2D_{5/2}$	6.28	
10	Pr^+	no	[Xe]4f^{14}5d^9	$^2D_{5/2}$	5.62	
11	Cu^+	no	[Ar]3d^{10}	$^1S_0$	6.89	2.70
11	Ag^+	no	[Kr]4d^{10}	$^1S_0$	7.04	
12	Zn^+	no	[Ar]4s3d^{10}	$^2S_{1/2}$	5.23	
12	Cd^+	no	[Kr]5s4d^{10}	$^2S_{1/2}$	5.63	

[a] The values of the reaction enthalpies for assumed charge-transfer reaction (ΔH_1) and F^- abstraction reaction (ΔH_2) are also listed which show that for these metal ions, every reaction 1 and some selected rection 2 (where auxiliary data are available) are all endothermic. [b] ΔH_1 = AP(SF_5^+/SF_6) − IP(M), where AP(SF_5^+/SF_6) = 14.62 eV[16] is the adopted value (see the text) and the IP values for each of the metals are obtained from ref 40. [c] ΔH_2 = [AP(SF_5^+/SF_6) − D(MF)] − IP(M). The values are listed for those reactions with available data in the literature to calculate *D*(MF). The auxiliary data used in the calculations are from refs 34 and 41. [d] SF_5^+ and SF_3^+ (predominant ion) were the observed products, but the reaction rate is less than 1×10^{-11} cm^3 molecules s^{-1} and, therefore, the reaction is believed to be slightly endothermic or have a slight kinetic barrier (see the discussion in section 3c of part II).

intensity increases. In addition, the reaction decay rates of the early transition metal ions are greater for hot ions than cooled ions due to the opening of endothermic reaction channels, as discussed below. Finally, it is worth pointing out that MF_m^+ products are also observed, where *m* can be up to the value of one less than the maximum oxidation number of the metal element.

1. Pathways of Cooled Sc^+ + SF_6. Reaction of Sc^+ with SF_6 produces ScF^+, ScF_2^+, and SF_n^+ (*n* = 2–5) (see Table III). In order to distinguish which are primary and secondary reaction products, the ScF^+, ScF_2^+, and SF_n^+ (*n* = 2–5) were each isolated after 1 s at a pressure of SF_6 of 1.5×10^{-7} Torr and then allowed to further react with SF_6 for 1 s. The results of the secondary reactions are shown below:

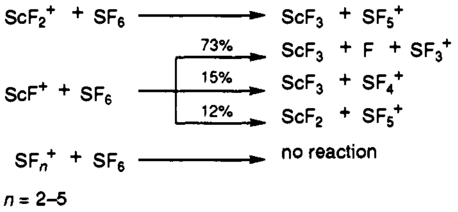

It is clear that while SF_n^+ cannot react with SF_6 and, therefore, are the terminal products, ScF^+ and ScF_2^+ are intermediates which can further react with SF_6 to form SF_n^+. There are no tertiary reactions. SF_2^+ is not found among the secondary products and, thus, it must be a primary product.

Continuous ejection of SF_n^+ (*n* = 2–5) causes little change in the intensities of the other ions, which is in accordance with the observation that SF_n^+ are unreactive with SF_6. As shown in Table IV, however, continuous ejection of ScF^+ or ScF_2^+ causes a change in the intensities of SF_3^+, SF_4^+, and SF_5^+. Continuously ejecting ScF^+ while allowing Sc^+ to react with SF_6 results in the intensity of SF_3^+ decreasing by 14%, implying that 86% of the SF_3^+ comes from Sc^+ directly. Similarly, it can be deduced that 59% of the SF_4^+ comes from the primary reaction of Sc^+. Surprisingly, an increase of 7% in the SF_5^+ intensity is observed when ScF^+ is continuously ejected, despite the fact that ScF^+ produces SF_5^+ from SF_6. An explanation for this behavior will be presented in section 3.

To provide further detail about the reaction pathways, some reaction enthalpies were calculated. Using the thermodynamic data in Table V, the calculations indicate that there is no exothermic path to generate SF_5^+ in the primary reaction of Sc^+ with SF_6. Also, in the primary reaction, the only exothermic paths to generate SF_4^+, SF_3^+, and SF_2^+, respectively are

$$Sc^+ + SF_6 \rightarrow ScF_2 + SF_4^+ \quad (\Delta H^\circ = -22.979\ \text{kJ/mol})$$

$$\rightarrow ScF_3 + SF_3^+ \quad (\Delta H^\circ = -650.19\ \text{kJ/mol})$$

$$\rightarrow ScF_3 + F + SF_2^+ \quad (\Delta H^\circ = -262\ \text{kJ/mol})$$

On the basis of the discussion above, the entire reaction scheme for Sc^+ reacting with SF_6 can be derived, as shown in Scheme I.

In Scheme I, paths 3, 4, 6, and 8 are the primary reactions while paths 7, 9, and 10 are the secondary reactions. Path 5 is considered to be a primary reaction, resulting from the autofragmentation of the primary product SF_3^+. Similarly, path 11 is considered as a secondary reaction. CID of SF_n^+ was performed and the results are presented in Table VI. Upon CID, SF_3^+ and SF_4^+ yield predominantly SF_2^+ and SF_3^+, respectively, supporting paths 5 and 11. It is interesting to note that some SF_5^+ is formed during the CID of SF_2^+, SF_3^+, or SF_4^+ arising from the background SF_6. Again, this will be discussed in section 3.

The enthalpies given for reactions 3–11 were calculated from the thermodynamic data in Table V. Among these data, the appearance potential for SF_5^+ is the least certain with several conflicting values reported in the literature, as summarized in a paper from Armentrout et al.[9h] These values, which have trended downward with time, span almost 2.5 eV, from 15.9 eV determined in 1948[32] and 1971[33] to 13.46 ± 0.15 eV determined by Armentrout and co-workers in 1992.[9h] Observation of reaction 9 implies that

$$\text{AP}(SF_5^+/SF_6) < \text{AP}(ScF^+/ScF_2) + 236.264\ \text{kJ/mol}$$

where the last term is the reaction enthalpy from eq 8, which is the maximum amount of energy that can be deposited in ScF^+ during its formation. From the heats of formation of F, ScF^+, and ScF_2 given in Table V, AP(ScF^+/ScF_2) = 1190.55 kJ/mol is obtained which, in turn, yields an upper limit of AP(SF_5^+/SF_6) < 1426.82 kJ/mol or 14.79 eV. On the other hand, as discussed below, path 7 is believed to be a "hot" reaction which yields a lower limit for AP(SF_5^+/SF_6). Although path 7 to form SF_5^+ from ScF_2^+ is believed to be endothermic, this reaction can occur because a large fraction of the reaction enthalpy from the primary reaction 6 is deposited into ScF_2^+ yielding a net negative total reaction enthalpy for eq 7. The evidence for this assertion can be clearly seen in the kinetics plot of the reactant intensity as a function of time, shown in Figure 1. For comparison, a kinetics plot for the reaction of ScF^+ with SF_6, which is itself exothermic and, thus, is not necessarily a hot ion reaction, is also shown in the figure. These two secondary reactions have different behaviors. For the ScF^+ reaction, the intensity of ScF^+ exhibits a single exponential behavior and approaches zero at long reaction times (Figure 1a), and the semilogarithmic plot gives a straight line (Figure 1b). For the ScF_2^+ reaction, however, biexponential behavior is seen in which the ScF_2^+ intensity begins to decay but

---

(32) Debeler, V. H.; Molhler, F. L. *J. Res. Natl. Bur. Stand.* **1948**, *40*, 25.

(33) Connolly, J. W. D.; Johnson, K. H. *Chem. Phys. Lett.* **1971**, *10*, 617.

(34) Chase, M. W., Jr.; Davies, C. A.; Downey, J. R., Jr.; Frurip, D. J.; McDonald, R. A.; Syverud, A. N. *JANAF Thermochemical Tables*; 3rd ed.; Journal of Physical and Chemical Reference Data, 1985; Vol. 14.

Table III. Product Distributions of Reactions of SF_6 and with Selected Early Transition Metal Ions

reactant	state	MF^+	MF_2^+	MF_3^+	MF_4^+	SF^+	SF_2^+	SF_3^+	SF_4^+	SF_5^+	$P(SF_6)$ (10^{-7} Torr)
Sc^+	cooled	5	20				47	20	2	6	1.5
	hot	6	20				43	19	2	10	1.5
Y^+	cooled	4	2				12	35		47	2.5
	hot	5	2				7	20		66	2.5
La^+	cooled	8	63				15	10		4	2.5
	hot	7	60				7	8		18	2.5
Ti^+	cooled	1	18	3			12	42	6	18	1.5
	hot	2	9	3			9	42	8	27	1.5
Zr^+	cooled	2	13	10		6	12	28	6	23	1.5
	hot	2	9	6		3	9	31	4	36	1.5
V^+	cooled		7		5			51	2	35	1.5
	hot	2	6		2		1	32	4	53	2.5
Nb^+	cooled		10	8	29	2	7	35	5	4	2.5
	hot	2	5	4	6		3	22	6	44	2.5
Ta^+	cooled	15	19	19	15		3	19	2	7	2.5
	hot	20	20	14	9			26		15	2.5

Table IV. Changes of Product Ion Intensities upon Double Resonance Ejection of ScF_2^+ and ScF^+

	changes of product ion intensities		
ions ejected	SF_3^+	SF_4^+	SF_5^+
ScF_2^+	no change	no change	decrease 90%
ScF^+	decrease 14%	decrease 41%	increase 7%

Table V. Thermodynamic Data for the Species Involved in the Sc^+ Reaction with SF_6

$\Delta H_f°$ (kJ/mol)[a]		$\Delta H_f°$ (kJ/mol)[a]		$\Delta H_f°$ (kJ/mol)[b]		IP (eV)[c]	
F	79.39	SF^+	991.901	Sc^+	1017.252	ScF^+	6.3
SF	12.970	SF_2^+	702.389	Sc	377.8	ScF_2^+	7.0
SF_2	−296.646	SF_3^+	393.589	ScF	−138.9		
SF_3	−503.303	SF_4^+	416.0	ScF_2	−642.2		
SF_4	−763.162	SF_5^+	172.644[d]	ScF_3	−1247		
SF_5	−908.447						
SF_6	−1220.473						

[a] Data are from ref 34. [b] Data are from ref 41. [c] Data are from ref 40. [d] Determined in this study to be 110.76 kJ/mol, calculated by using the value for AP(SF_5^+/SF_6) as 14.62 eV. See the text.

then levels off after 1.5 s (Figure 1c). This is due to the fact that some of the internally hot ScF_2^+ ions are cooled down by collisions with Ar and SF_6 during the reaction time and, for some ScF_2^+ ions, insufficient energy has been deposited from reaction 6. Given that reaction 7 is endothermic itself, the lower limit for AP(SF_5^+/SF_6) is

$$AP(SF_5^+/SF_6) > AP(ScF_2^+/ScF_3)$$

The right-hand side of the above equation is calculated using the auxiliary data in Table V to be 14.1 ± 0.3 eV. The error bar arises predominantly from the value of IP(ScF_2^+), 7.0 ± 0.3 eV. This lower limit is higher than the value of 13.46 ± 0.15 eV recommended by Armentrout et al.[9h] Thus, in the calculations elsewhere in this paper, we have chosen to adopt 14.62 ± 0.09 eV determined by Babcock and Streit,[16] which has been the most widely accepted value recently. On the basis of this value, the net reaction enthalpy for eq 7 is calculated to be −475.71 kJ/mol, and that for eq 9 is −16.19 kJ/mol.

It is interesting to note that while the ScF^+ reaction generates SF_4^+ (path 10), which can further fragment to form SF_3^+, the hot ScF_2^+ reaction generates SF_5^+, which does not further fragment to form either SF_4^+ or SF_3^+. This is despite the thermodynamic calculations which, assuming that the entire reaction enthalpy of eq 7 (−475.71 kJ/mol) is deposited into SF_5^+, indicate that the following fragmentations can occur:

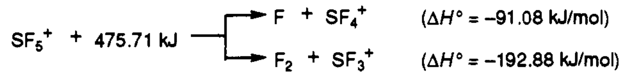

$$SF_5^+ + 475.71\ \text{kJ} \rightarrow \begin{cases} F + SF_4^+ & (\Delta H° = -91.08\ \text{kJ/mol}) \\ F_2 + SF_3^+ & (\Delta H° = -192.88\ \text{kJ/mol}) \end{cases}$$

This observation suggests that the reaction of hot ScF_2^+ with SF_6 to form ScF_3 and SF_5^+ (eq 7) proceeds through the mechanism of F^- abstraction. As a result, the extra energy of reaction 7 is deposited into the new bond formed in ScF_3 and, thus, SF_5^+ does not have enough energy to fragment.

The fact that SF_n^+ ions were not observed to undergo secondary reactions with SF_6 is in accordance with the thermodynamic calculations which indicate that any reaction of SF_n^+ with SF_6 is endothermic. For these reactions to occur, the reactants SF_n^+ must be hot which is possible if they obtain energy from the primary reaction enthalpies. For example, if the reaction enthalpy of eq 4 (−650.19 kJ/mol) is deposited into SF_3^+, the following reaction could occur according to its exothermicity:

$$SF_3^+ + SF_6 + 650.19\ \text{kJ/mol} \rightarrow SF_4 + SF_5^+ \quad (\Delta H° = -475.71\ \text{kJ/mol})$$

However, this is not observed. Either insufficient reaction enthalpy is deposited into the SF_3^+ ions or, when enough energy is deposited from reaction 4, they simply autofragment to form SF_2^+ (path 5).

2. $[MSF_6]^+$ Mechanism. The reaction scheme discussed in section 1 reveals two important features: First, every possible exothermic primary reaction, namely, eqs 3, 4 (and 5), 6, and 8, occurs, indicating that there is essentially no kinetic barrier in the reaction of SF_6 with Sc^+. Second, this reaction is different and more complex than the reactions of SF_6 with non-metal ionic species, X^+, listed in Table I, which mainly produce SF_5^+. In those cases, X^+ cannot attack the S atom in SF_6; instead it can only extract either one electron or F^-, as described in eqs 1 and 2. When Sc^+ reacts with SF_6 by the reaction paths shown above, however, the mechanism cannot simply be explained by a charge tranfer or F^- abstraction. Instead, the formation of ScF_2^+ as a *primary* product implies that the mechanism must involve a long-lived $[Sc\cdots SF_6]^+$ intermediate within which F transfer from S to Sc takes place, as shown below:

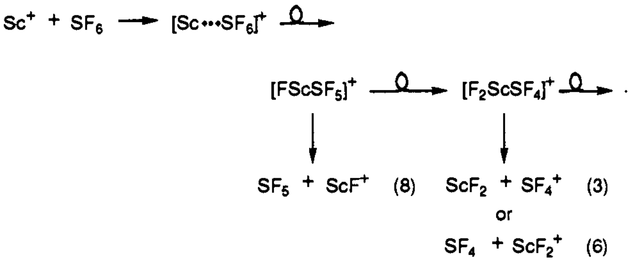

Simple molecular orbital (MO) ideas can be used to help understand the mechanism by which Sc^+ can attack the sulfur center. As mentioned in the introduction, whether the 3d orbitals of the S atom participate in the bonding orbitals of SF_6 is still

Scheme I

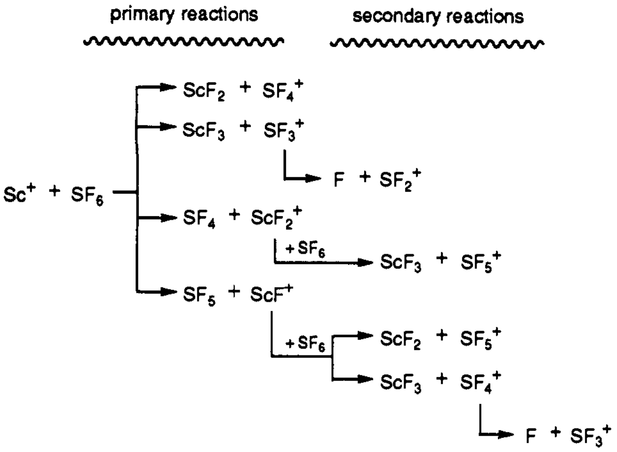

	ΔH° (kJ/mol)	branching ratio (%)[a]	
$ScF_2 + SF_4^+$	-22.979	1	(3)
$ScF_3 + SF_3^+$	-650.19	16	(4)
$F + SF_2^+$	-262	43	(5)
$SF_4 + ScF_2^+$	-526.739	20	(6)
$ScF_3 + SF_5^+$	-475.71	9	(7)
$SF_5 + ScF^+$	-236.264	6	(8)
$ScF_2 + SF_5^+$	-16.19	1	(9)
$ScF_3 + SF_4^+$	-315.753	1	(10)
$F + SF_3^+$	-258.774	3	(11)

[a] Relative branching ratios derived after 1 s reaction time. See section 3.

a matter of debate. Here we consider these 3d orbitals to be taking part in the MO of SF_6. One of the e_g molecular orbitals is shown on the left of Figure 2.[8] $Z_1, Z_2, ..., Z_4$ represent one of the two sp hybrids (directed at the S atom) of each of the four F atoms, $F_1, F_2, ..., F_4$, respectively. The subscript numbers denote the F atom positions around the S atom as shown in the figure. The e_g orbital is an occupied bonding orbital and can play an important role in SF_6 chemistry. While new bonding to the S atom is blocked along the directions of the F atoms, an attacking reagent with an empty d orbital of the proper symmetry, on the other hand, can readily approach in the space between the F atoms and form a bond through the e_g orbital of SF_6, as shown on the right in Figure 2.

The early transition metal ions have at least one empty d orbital available and so can readily react with SF_6, directly attacking the S atom to form the long-lived complex $[M\cdots SF_6]^+$. Insertion, F atom transfer, and elimination then occur, producing an overall product distribution much different from that seen for the non-metal ions which cannot attack the S atom. The failure of the late transition metal ions in their ground states to react with SF_6 can now be understood. It is surely not due to thermodynamic factors. For example, for Sc^+, the following reaction occurs with a reaction rate of 2.7×10^{-10} cm^3 molecules^{-1} s^{-1}:

$$Sc^+ + SF_6 \rightarrow ScF_3 + SF_3^+ \quad (\Delta H = -650.19 \text{ kJ/mol}) \quad (2)$$

but the analogous reaction for Fe^+, even though it is also exothermic, is rather slow with a reaction rate of about 7×10^{-12} cm^3 molecules^{-1} s^{-1}.

$$Fe^+ + SF_6 \rightarrow FeF_3 + SF_3^+$$

$$(\Delta H = -648.231 \text{ kJ/mol; calculated from data in ref 34})$$

And for Co^+, the reaction is not observed at all:

$$Co^+ + SF_6 \rightarrow CoF_3 + SF_3^+$$

$$(\Delta H = -367.898 \text{ kJ/mol; calculated from data in ref 34})$$

Thus, the reduced reactivity must arise due to kinetic factors. Late transition metal ions in their ground states have no empty d orbitals available to form the long-lived $[M\cdots SF_6]^+$ complex; instead, they can only form an ion–induced-dipole complex, $[M^+\cdots SF_6]$. In order for the metal ions to prepare an empty d orbital, one electron must be promoted to a higher energy orbital, resulting in a significant energy barrier.

For the late transition metal ions, the reaction with SF_6 can follow the types of mechanisms seen for the non-metal ionic species, such as charge transfer and F^- transfer. But, since these reactions require IP(M) > AP(SF_5^+/SF_6) (for reaction 1) or IP(M) > [AP(SF_5^+/SF_6) − *D*(XF)] (for reaction 2), they cannot occur when the metal ions are in the ground state.

When the early transition metal ions are kinetically hot, they can also react with SF_6 by the mechanism of charge transfer or F^- abstraction which produces predominantly SF_5^+, as well as by the long-lived $[Sc\cdots SF_6]^+$ mechanism. This would explain why the intensities of SF_5^+ in the product distributions are higher when the metal ions are hot than when they are cooled. It would also explain why the hot early transition metal ions react with SF_6 at a greater rate than the cooled ones. The high-energy metal ions have two reaction channels (although the exothermic reaction channels slow down as the reactant gets hotter), while the cooled metal ions only have one.

3. Reaction Branching Ratios. An estimate of the branching ratios for reactions 3–11 can be obtained from double resonance experiments on ScF_2^+ and ScF^+. The changes in product ion intensities upon continuously ejecting these two ions are shown in Table IV. As stated earlier, the data indicate that 14% of the SF_3^+ comes from ScF^+ by reaction 11 and 86% of the SF_3^+ is from reaction 4. The total normalized intensity of SF_3^+ after the 1 s of reaction time is 19%; thus, the branching ratio for reaction 11 is 3% and that of reaction 4 is 16%. In a similar fashion, we estimate that the branching ratios for reactions 3 and 10 to produce SF_4^+ are both 1%. Branching ratios for reactions 5, 6, and 8 can be directly obtained from the normalized intensities of SF_2^+, ScF_2^+, and ScF^+ which are 43%, 20%, and 6%, respectively, since they are the only reactions to generate these ions. A summary of the product branching ratios is shown along with reactions 3–11.

We now consider the observation, discussed earlier, that when double resonance ejection is performed on ScF^+, the intensity of SF_5^+ increases. Instead, it should decrease since some of the SF_5^+ comes directly from ScF^+. Our explanation for this is that when ScF^+ is continuously ejected, a small portion of the kinetically excited ScF^+ ions reacts with SF_6 through the mechanism of charge transfer. Charge transfer reactions can occur by a long-range electron jump mechanism which results in a larger reaction rate than the calculated collision rate.[22] Apparently, although the duration of the ScF^+ being ejected is short, it can still produce a small but measurable amount of SF_5^+. Similarly, the appearance of small amounts of SF_5^+ in the CID of SF_4^+, SF_3^+, and SF_2^+ in Table VI can also be explained. Upon CID, these ions become kinetically hot and can react with SF_6 by charge transfer or F^- abstraction to produce SF_5^+.

This phenomenon makes it difficult to estimate the branching ratios for reactions 7 and 9. However, a reasonable estimate can be made by ignoring these small perturbations and basing it on the observation of a 90% decrease of SF_5^+ when ScF_2^+ is continuously ejected. Combined with the total intensity of SF_5^+ being 10%, this results in a branching ratio of 9% for reaction 5 and 1% for reaction 7.

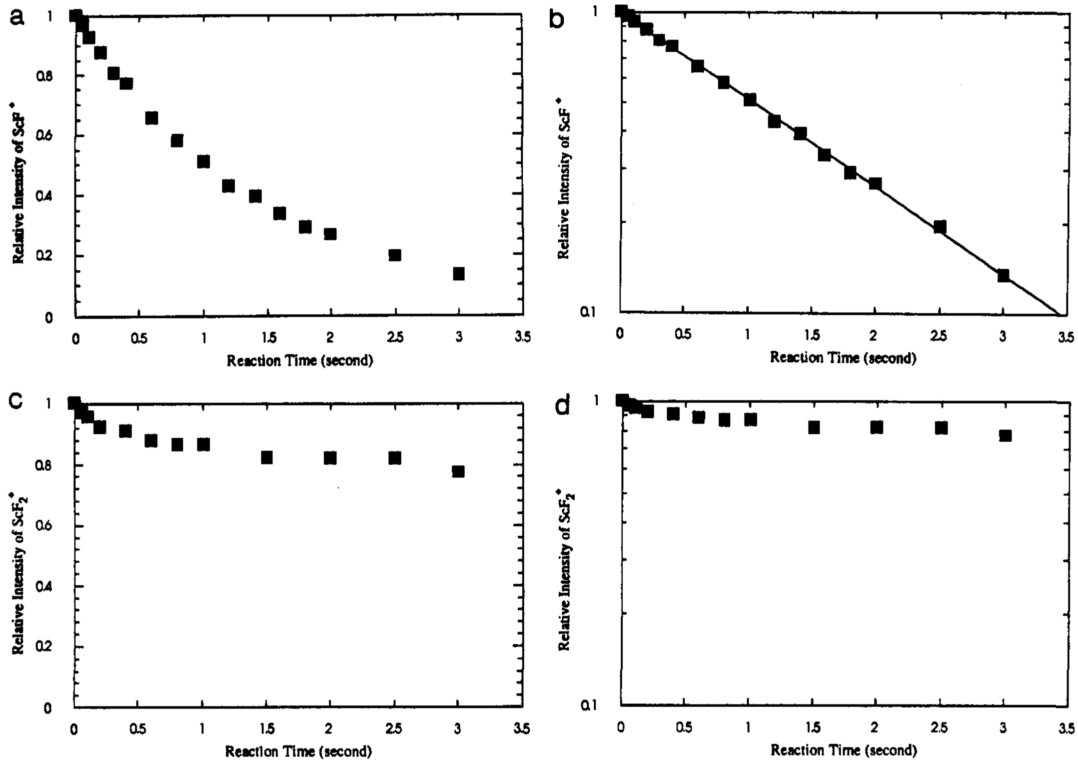

Figure 1. (a) Plot of ScF$^+$ intensity vs reaction time at 1.5 × 10^{-7} Torr of SF$_6$. (b) Semilogarithmic plot for the ScF$^+$ reaction. (c) Plot of ScF$_2^+$ intensity vs reaction time at 1.5 × 10^{-7} Torr of SF$_6$. (d) Semilogarithmic plot for the ScF$_2^+$ reaction.

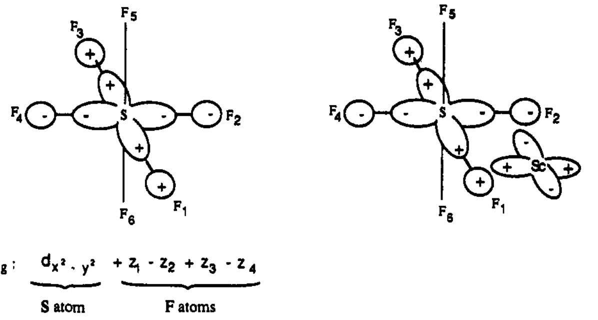

Figure 2. Left: Orbital diagram for one of the e_g molecular orbitals of SF$_6$. Right: Orbital interaction between an empty 3d orbital of Sc$^+$ with the e_g orbital of SF$_6$.

Table VI. Products of CID on SF$_n^+$ Ions

reactant ion	KE(max) (eV)	product ions^a SF$^+$	SF$_2^+$	SF$_3^+$	SF$_4^+$	SF$_5^+$
SF$_2^+$	60	61				39
SF$_3^+$	47	11	76			13
SF$_4^+$	39		5	86		9
SF$_5^+$	66		8	87	5	

^{a} The values shown are the normalized relative intensities of product ions.

Although the percentages obtained are not highly accurate, their reliability is good enough for the following discussion.

(A) SF$_4^+$ and ScF$_2^+$ are formed in a competitive manner as shown in the following sequence:

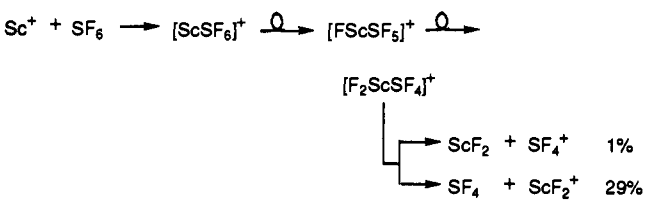

Note that the branching ratio for the formation of ScF$_2^+$ is the sum from reactions 6 and 7. The ionization potentials of SF$_4$ and ScF$_2$ are 12.22 and 7.00 eV, respectively. This lends support to the mechanism of a long-lived [ScSF$_6$]$^+$ which fragments to give mainly ScF$_2^+$ and SF$_4$ in accordance with Stevenson's rule.[35] For the X$^+$ reaction (in Table I), on the other hand, the products are not from [XSF$_6$]$^+$, and Stevenson's rule is sometimes not observed. For example, in the reactions of CO$^+$ and C$^+$, despite the ionization potentials for COF (8.76 ± 0.32 eV) and CF (9.11 ± 0.01 eV)[36] being lower than that of SF$_5$ (10.56 ± 0.1 eV), the only product ion is SF$_5^+$. A similar analysis for observing Stevenson's rule in the product ion ScF$^+$ (reaction 6) and its hypothetical competitive product SF$_5^+$, or the product ion SF$_3^+$ (reaction 2) and its hypothetical competitive product ScF$_3^+$, is not necessary because in the first case the production of SF$_5^+$ is endothermic and not possible and in the second case the ScF$_3^+$ ion cannot be formed at all since the oxidation number of Sc in this species exceeds the allowed value.

(B) An inspection of the branching ratios for reactions 5, 7, and 11 can provide a rough estimate of the fractions of the product ions to which a certain amount of reaction enthalpy has been deposited. By comparing the ratios for reactions 4 and 5, for example, it is apparent that about 73% of the SF$_3^+$ has obtained more than 388 kJ/mol from reaction 4. Similarly, 75% of SF$_4^+$ retains more than 57.0 kJ/mol from reaction 10. In reaction 6, apparently only about 30% of the product ion ScF$_2^+$ is hot enough to undergo reaction 7. The actual value should be greater than that, since a portion of these hot ScF$_2^+$ ions is cooled down by collisions with Ar during the reaction time for eq 7. Finally, 0% of SF$_5^+$ in eq 7 retains more than 282.8 kJ/mol (the energy required to break SF$_5^+$ into SF$_3^+$ and F$_2$, the lowest energy fragmentation of SF$_5^+$) from reaction 7, since no SF$_5^+$ undergoes further fragmentation. One explanation for this was presented in section 1.

---

[35] Stevenson, D. P. *Discuss. Faraday Soc.* **1951**, *10*, 35.

[36] Lias, S. G.; Bartmess, J. E.; Liebman, J. F.; Holmes, J. L.; Levin, R. D.; Mallard, W. G. *Gas-Phase Ion and Neutral Thermochemistry*; Journal of Physical and Chemical Reference Data, 1988; Vol. 17.

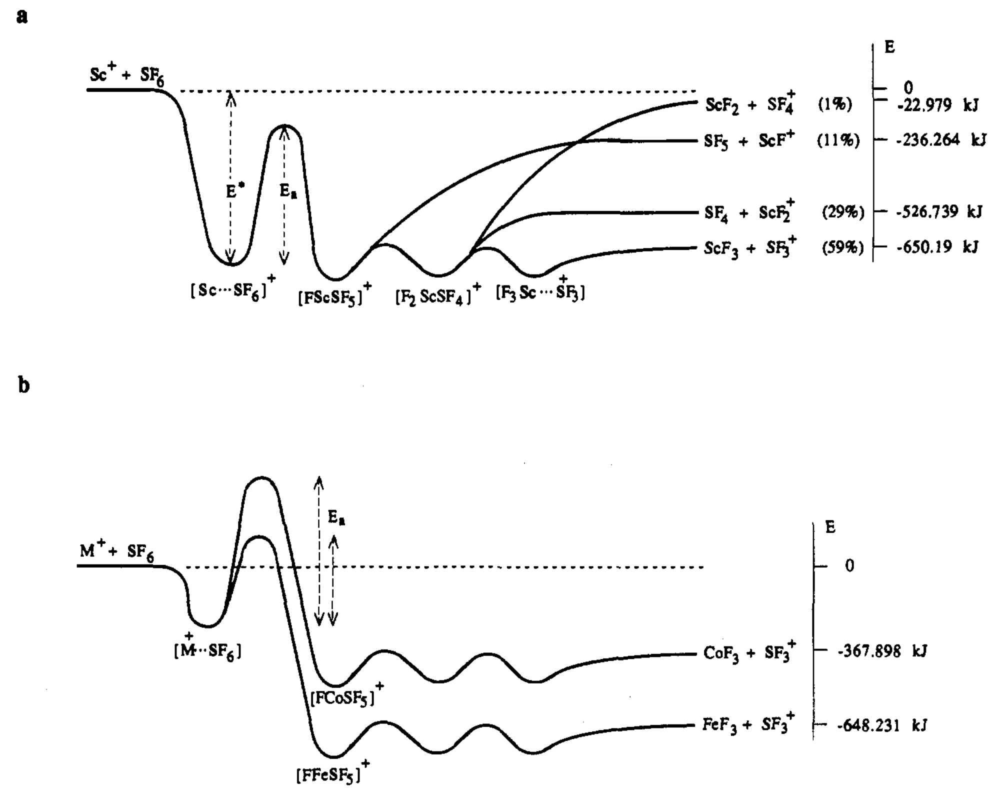

Figure 3. (a) Potential energy surface diagram for the reaction of Sc^+ with SF_6. (b) Potential energy surface diagrams for Co^+ and Fe^+ reaction with SF_6.

(C) The whole reaction takes place through four channels, namely, reactions 3, 4, 6, and 8, which are expressed in the following equations:

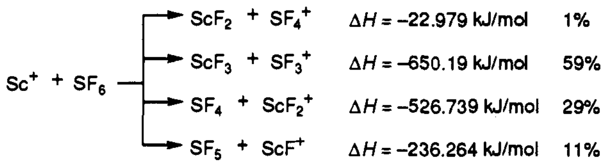

$Sc^+ + SF_6 \rightarrow ScF_2 + SF_4^+$ $\Delta H = -22.979$ kJ/mol 1%
$Sc^+ + SF_6 \rightarrow ScF_3 + SF_3^+$ $\Delta H = -650.19$ kJ/mol 59%
$Sc^+ + SF_6 \rightarrow SF_4 + ScF_2^+$ $\Delta H = -526.739$ kJ/mol 29%
$Sc^+ + SF_6 \rightarrow SF_5 + ScF^+$ $\Delta H = -236.264$ kJ/mol 11%

The reaction enthalpies and the normalized branching ratios are also shown (the percentage shown for each path is from the sum of the intensities of ions which are generated through the given channel). The reaction involves an initial interaction of Sc^+ with SF_6 and the insertion of Sc^+ into an S–F bond, followed by successive F transfers from the S atom to the Sc atom. The reaction system exits by dissociation of the Sc–S bond. A dissociation step can occur at different stages of the reaction and, thus, different product ions are formed. From the above equations, it can be seen that the branching ratios track the reaction enthalpies. This relationship suggests that the dissociation step controls the product distribution. A qualitative diagram of the potential energy surface for the reactions is shown in the top part of Figure 3. The first step of the reaction is the forming of the $[Sc\cdots SF_6]^+$ complex by the orbital interaction discussed earlier. Since this complex has sufficient internal energy (E^*) to overcome an activation barrier (E_a) to form the bond-insertion intermediate, $[FScSF_5]^+$, this second step, from $[Sc\cdots SF_6]^+$ to $[FScSF_5]^+$, is facile. Likewise, $[FScSF_5]^+$ can dissociate to form the ionic product ScF^+ or it can convert to another intermediate, $[F_2ScSF_4]^+$, which can then dissociate through two competitive channels to form SF_4^+ or ScF_2^+, or further convert to $[F_3Sc\cdots SF_3]^+$ followed by dissociation to form SF_3^+. The barriers for each conversion between $[FScSF_5]^+$, $[F_2ScSF_4]^+$, and $[F_3Sc\cdots SF_3]^+$ are relatively small and, thus, the relative reaction rate for each channel is determined by the barriers for the dissociations. These barriers are proportional to the heats of reactions for each product pair formation, as is also indicated in the figure.

For comparison, a typical diagram of the potential energy surface for the late transition metal ion reactions is represented for Co^+ and Fe^+, plotted in the bottom part of the figure. Since Co^+ has no empty d orbital, it can only form the ion–induced-dipole complex, $[Co^+\cdots SF_6]$, which does not have enough internal energy to overcome the activation barrier (E_a) to form the oxidative addition intermediate $[FCoSF_5]^+$. The activation barrier (E_a) may vary depending on the metal ions. For Fe^+, it is apparently lower than for Co^+, which is reflected by its rather low but observable reaction rate. When the kinetic energies of M^+ are high enough, all of the metal ions, including the late transition metal ions, can react with SF_6, not through the formation of $[FMSF_5]^+$, but by direct charge transfer to form $[SF_6^+]^*$ or by F^- abstraction to form SF_5^+.

4. Reaction Rate Constants. For all of the early transition metal ion reactions, the potential energy diagrams should be similar to that for the Sc^+ reaction in Figure 3. The efficiency of the reaction upon each collision depends on the possibility of forming $[M\cdots SF_6]^+$, as well as the activation barrier E_a. If the barrier is high, $[M\cdots SF_6]^+$ will tend to fall apart back to the reactants, instead of advancing to $[MFSF_5]^+$. Rate constants for the early transition metal ion reactions were determined and are listed in Table VII. To calculate these second-order reaction rate constants from the measured pseudo-first-order reaction rates, the absolute pressures of SF_6 were calibrated as discussed in the Experimental Section. Collision rate constants for each reaction were calculated from Langevin theory, using 6.54 Å^3 for the polarizability of SF_6.[22]

From Table VII it can be seen that the reaction efficiencies are, surprisingly, all about the same for the tested reactions, except for V^+ and Nb^+, which are less than half of that for the other ions. While the IP values (also listed in the table) for these metals cannot explain the behavior of the V^+ and Nb^+, the electron configuration may be the key factor. One possibilty is that since V^+ and Nb^+ have fewer empty d orbitals than the other ions, their reaction wth SF_6 is less likely to occur. This explanation, however, fails to explain why all of the other early transition metal ions have about the same reaction efficiencies, even though

Table VII. Experimental and Theoretical Rate Constants for the Reactions of Early Transition Metal Ions (M^+) with SF_6

M^+	k_{exptl} (10^{-10} cm^3 s^{-1})	k_{calcd} (10^{-10} cm^3 s^{-1})	$k_{\text{exptl}}/k_{\text{calcd}}$	IP (eV)[b]			electron configuration[c]	
				I	II	III		
Sc^+	2.7	10	0.27	6.54	12.80	24.76	[Ar]4s3d	$^3D_1$
Y^+	2.3	8.1	0.28	6.38	12.24	20.52	[Kr]$5s^2$	$^1S_0$
La^+	1.8	7.1	0.25	5.577	11.06	19.175	[Xe]$5d^2$	$^3F_2$
Ti^+	2.4	10	0.24	6.82	13.58	27.491	[Ar]$4s3d^2$	$^4F_{3/2}$
Zr^+	2.1	8.0	0.26	6.84	13.13	22.99	[Kr]$5s4d^2$	$^4F_{3/2}$
V^+	0.86	9.7	0.09	6.74	14.65	29.31	[Ar]$3d^4$	$^5D_0$
Nb^+	0.87	7.9	0.11	6.88	14.32	25.04	[Kr]$4d^4$	$^5D_0$
Ta^+	1.7	6.7	0.25	7.89			[Xe]$4f^{14}6s5d^3$	$^5F_1$

[a] Overall reaction efficiency. [b] These data are cited from ref 42. [c] Cited from ref 43.

Y^+, for example, has five empty d orbitals while Ta^+ only has two empty d orbitals. Thus, two alternative explanations are proposed.

Of the five d orbitals, all but the d_{z^2} have the proper symmetry to interact with the e_g orbital of SF_6. V^+ and Nb^+ have only one empty d orbital each and, if it happens to be the d_{z^2} orbital, the reaction cannot occur. For each of the other ions in Table VII, however, there is more than one empty d orbital. Thus, even if the d_{z^2} orbital is empty, there is at least one additional orbital of the correct symmetry which is empty, permitting the efficient formation of the long-lived intermediate, $[M\cdots SF_6]^+$. The reaction efficiencies of V^+ and Nb^+ are about one-half to one-third of that for the other ions, instead of the four-fifths expected assuming that there is an equal probability for any of the five d orbitals to be empty. This suggests that when the metal ions and SF_6 approach each other, the d orbital energies split, making the empty d_{z^2} more favored and, thus, the reaction less likely to occur. Finally, another reasonable explanation is that, assuming that the S–F insertion energies for these metal ions are more or less about the same, V^+ and Nb^+ could have lower reaction efficiencies because their exchange and promotional energies for the formation of two covalent bonds are higher than those for the other early transition metal ions.[37]

IV. Summary

The inertness of SF_6 is due to kinetic factors, specifically, the protecting F atom layer around the S atom which makes direct attack on S by reagents difficult. When SF_6 reacts with ions which have relatively high IP values, SF_6 can undergo charge transfer or F^- abstraction, as studied previously. This work has shown that when SF_6 reacts with early transition metal ions, such as Sc^+, a different mechanism is involved as evidenced by the observation of a different product pattern. In particular the reaction of Sc^+ with SF_6 reveals multiple reaction paths, with ScF^+ and ScF_2^+ as intermediate products, and SF_n^+ (n = 2–5) as terminal products, formed from both primary reactions and secondary reactions. We propose that the mechanism proceeds through the formation of a long-lived intermediate, $[Sc\cdots SF_6]^+$, in which F transfers from the S atom to the Sc atom can occur. $[Sc\cdots SF_6]^+$ is formed by direct attack on the S atom by early transition metal ions which have at least one empty d orbital available. In support of this argument is the trend of the reaction rate efficiencies for the different metal ions, where the absence of an empty d orbital results in a greatly reduced efficiency. Finally, this study shows that reaction of SF_6 with early transition metal ions is an efficient way to break down the S–F bond in SF_6.

Acknowledgment is made to the Division of Chemical Sciences in the Office of Basic Energy Sciences in the United States Department of Energy (DE-FG02-87ER13766) for supporting this research and to the National Science Foundation (CHE-8920085) for providing funds for the advancement of FTMS methodology. We also thank Dr. Charles W. Bauschlicher, Jr., and Dr. Lee Sunderlin for their helpful comments and suggestions.

---

(37) Carter, E. A.; Goddard, W. A., III *J. Phys. Chem.* **1988**, *92*, 5679.

(38) Fehsenfeld, F. C. *J. Chem. Phys.* **1971**, *54*, 438.

(39) Richter, R.; Tosi, P.; Lindinger, W. *J. Chem. Phys.* **1987**, *87*, 4615.

(40) Rosenstock, H. M.; Draxl, K.; Steiner, B. W.; Herron, J. T. *Energetics of Gaseous Ions*; Journal of Physical and Chemical Reference Data, 1977; Vol. 6.

(41) Wagman, D. D.; Evans, W. H.; Parker, V. B. Schumm, R. H.; Halow, I.; Bailey, S. M.; Churney, K. L.; Nuttall, R. L. *The NBS Tables of Chemical Thermodynamic Properties*; Journal of Physical and Chemical Reference Data, 1982; Vol. 11.

(42) *CRC Handbook of Chemistry and Physics*, 66th ed.; Weast R. C., Ed.; CRC Press: Boca Raton, FL, 1985.

(43) Moore, C. E. *Atomic Energy Levels*; U.S. National Bureau of Standards: Washington, DC, 1948, 1952, 1958; Circular 467 (U.S. National Bureau of Standards).

(44) Russell, D. H.; Oriedo, J. V. B. *J. Phys. Chem.* **1992**, *96*, 5314.